Nuclear Instruments and Methods in Physics Research A 659 (2011) 368–372

Contents lists available at SciVerse ScienceDirect

Nuclear Instruments and Methods in Physics Research A

journal homepage: www.elsevier.com/locate/nima

Crystal growth and scintillation properties of Ce and Eu doped $LiSrAlF_6$

Akihiro Yamaji [a,*], Takayuki Yanagida [b], Noriaki Kawaguchi [c], Yutaka Fujimoto [a], Yuui Yokota [a], Kenichi Watanabe [d], Atsushi Yamazaki [d], Akira Yoshikawa [a,b], Jan Pejchal [e]

[a] Institute of Materials Research, Tohoku University, 2-1-1 Katahira, Aoba-ku, Sendai 980-8577, Japan
[b] New Industry Creation Hatchery Center (NICHe), Tohoku University, 6-6-10 Aoba, Aramaki, Aoba-ku, Sendai 980-8579, Japan
[c] Tokuyama Corporation, Shibuya 3-chome, Shibuya, Tokyo 150-8383, Japan
[d] Department of Material, Physics and Energy Engineering, Nagoya University, Furo-cho, Chikusa-ku, Nagoya, 464-8603, Japan
[e] Institute of Physics AS CR, Cukrovarnicka 10, 16200 Prague 6, Czech Republic

ARTICLE INFO

Article history:
Received 11 July 2011
Received in revised form
22 August 2011
Accepted 25 August 2011
Available online 1 September 2011

Keywords:
$LiSrAlF_6$
Single crystal
Scintillation detector
Neutron
Scintillator

ABSTRACT

Ce and Eu doped $LiSrAlF_6$ (LiSAF) single crystals for the neutron detection with different dopant concentrations were grown by the micro-pulling-down method (μ-PD). In Ce:LiSAF, intense emission peaks due to Ce^{3+} 5d–4f transitions were observed at approximately 315 and 335 nm in photo- and α-ray induced radio-luminescence spectra. In case of Eu:LiSAFs, an intense emission peak at 375 nm due to Eu^{2+} 5d–4f transition was observed in the radio-luminescence spectra. The pulse height spectra and decay time profiles were measured under ^{252}Cf neutron irradiation to examine the neutron response. The Ce 3% and Eu 2% doped LiSAF showed the highest light yield of 2860 ph/n with 19 ns main decay time component and 24,000 ph/n with 1610 ns.

1. Introduction

Inorganic scintillation materials are widely used in many fields of radiation detection. Recently, the scintillation materials for therma neutron detection have attracted much attention as an alternative to ^3He gas filled proportional counters. The ^3He gas filled proportional counters with high thermal neutron cross-section and low background γ-ray sensitivity have been widely used in the thermal neutron detectors. However, ^3He sources are gradually getting depleted [1]. For this reason, alternative techniques for neutron detection are required. Recently, we developed new scintillators, Ce:$LiCaAlF_6$ (LiCAF) [2,3] and Eu:LiCAF [4] single crystals, for thermal neutron detectors, because they have a high cross-section for thermal neutrons due to $^6Li(n, \alpha)^3H$ reaction and low γ-ray sensitivity due to low effective atomic number of 15. When ^{252}Cf excited pulse height spectra were measured, the Ce:LiCAF showed medium light yield (3500 ph/n) and very fast decay time (40 ns) and the Eu:LiCAF exhibited high light yield (29,000 ph/n) and a slightly slower decay time (1.15 μs). In addition, both of them are not hygroscopic and can be grown as a large size single-crystal.

Recently, we examined neutron response of Ce 1%LiSAF and Eu 1, 2%:LiSAF to investigate their capabilities for neutron detection [5]. The LiSAF is a host material analogous to $LiCaAlF_6$ where Ca^{2+} is fully substituted by Sr^{2+}. Since the ionic radius of Sr^{2+} is closer to Eu^{2+} than that of Ca^{2+}, it is expected that the dopant concentration in the crystal can be increased. In our last results, the Ce- and Eu-doped LiSAFs showed scintillation properties comparable to the LiCAFs. Our previous studies have focused on the optical properties of these materials including absorption and emission spectra [6–8], but the scintillation properties of LiSAF with different Ce and Eu doping concentrations have not been reported yet.

In this work, we grew Ce^{3+} and Eu^{2+} doped $LiSrAlF_6$ (LiSAF) single crystals with different dopant concentrations. After the crystal growth, we systematically evaluated their optical properties, α-ray induced radio luminescence, and neutron response.

2. Crystal growth

Single crystals with nominal chemical compositions of $Li(Sr_{1-x}Ce_x)AlF_6$ and $Li(Sr_{1-y}Eu_y)AlF_6$ were grown by the micro-pulling-down (μ-PD) method [9]. The starting materials were prepared from the stoichiometric mixture of 4 N pure LiF (95% ^6Li), SrF_2, AlF_3, CeF_3 and EuF_3. They were thoroughly mixed and put into a graphite crucible. After the installation of the crucible into the chamber in the growth furnace, the chamber was

* Corresponding author.
E-mail address: yamaji-a@imr.tohoku.ac.jp (A. Yamaji).

0168-9002/$ - see front matter © 2011 Elsevier B.V. All rights reserved.
doi:10.1016/j.nima.2011.08.048

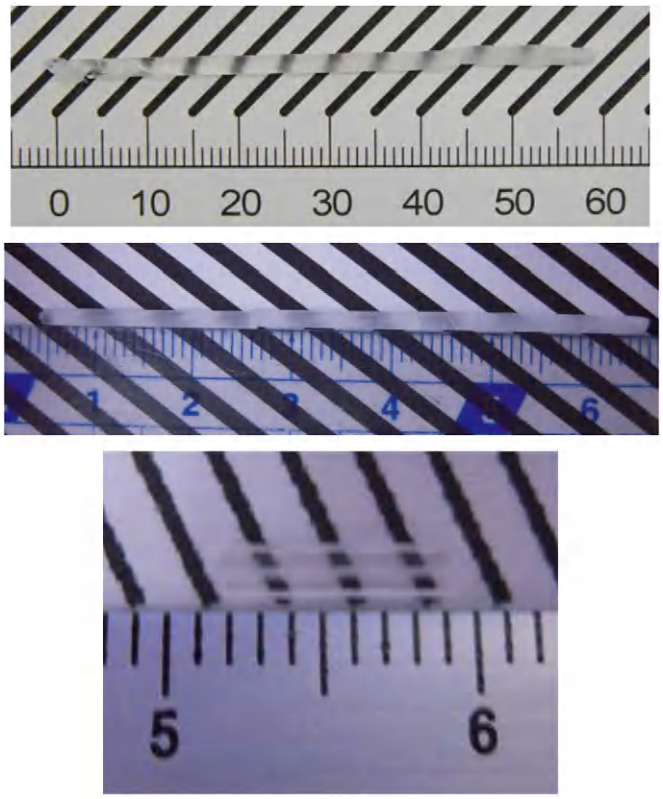

Fig. 1. Photograph of as-grown Ce:LiSAF (upper) and Eu:LiSAF (middle) single crystals. The cross-section of Eu 3%:LiSAF (bottom) crystals along the growth direction. The obtained crystals had milky portions in the center of the crystals.

evacuated up to 10^{-3} Pa. Then, the crucible was heated up to 400 °C and kept for about 1 h at this temperature in order to remove oxygen traces caused by moisture of raw materials and adsorbates on the chamber surface. During this baking procedure, the chamber was further evacuated down to 10^{-4} Pa. After the baking, the recipient was filled with high purity Ar and CF_4 atmosphere until the ambient pressure. Finally, the crucible was heated up to the melting temperature of LiSAF. A platinum wire was used as the seed for initial crystal growth and the crystal growth rate was 0.1 mm/min.

Using such crystal growth procedure, the Ce 0.25, 0.50, 1.5, 2.0 and 3.0 mol% doped and the Eu 0.25, 0.50, 1.0, 2.0, 3.0 and 4.0 mol% doped LiSAF single crystals were successfully obtained. The as-grown crack-free Ce:LiSAF single-crystals had 2 mm in diameter and 40–60 mm in length , as shown in Fig. 1. However, when we the dopant concentration was increased, some parts of the obtained crystals had milky parts in the center of the crystals and were not transparent enough. This was due to the existence of a secondary phase. These secondary phases were identified as CeF_3 in Ce:LiSAF and EuF_2 in Eu:LiSAF phases confirmed by powder X-ray diffraction. The fabricated crystals were cut and polished to get samples for optical characterization of typical dimensions of $2 \times 7 \times 1$ mm^3.

3. Photoluminescence

Photoluminescence spectra were recorded by a modified spectrofluorimeter (FLS920 Edinburgh Instruments). A Xenon arc lamp was used for the excitation and emission spectra measurements. A steady-state hydrogen nanosecond flashlamp was used for the photoluminescence decay measurements using the method of time-correlated single photon counting. Fig. 2 presents emission spectra of Ce:LiSAF and Eu:LiSAF excited by 280 nm and 330 nm, respectively, for various concentrations of the dopants. The emission peaks for the Ce:LiSAF appeared at approximately 315 nm and 335 nm due to Ce^{3+} 5d–4f related transitions and they were very similar to those of Ce:LiCAF. The segregation coefficient of Ce is smaller than that of Eu and the secondary phase of CeF_3 in Ce:LiSAF affected the emission properties. The CeF_3 microphase might be contaminated by divalent Sr^{2+}, which leads to enchanced Ce-perturbed emission known in CeF_3 to occur at longer wavelength [10,11]. For this reason, the emission peaks shifted to the longer wavelength in high Ce dopant concentrations. The emission peak for Eu:LiSAF appeared at approximately 375 nm due to the Eu^{2+} 5d–4f-related transition. The Eu:LiSAF was less affected by the secondary phase than Ce:LiSAF, due to the above-mentioned difference of the segregation coefficients of both dopants. The photoluminescence decay times of Ce: LiSAF and Eu:LiSAF are displayed in Fig. 4 as a function of the dopants concentrations. In both material systems, the decay times were almost constant with the concentrations of the dopants. The decay time of Ce:LiSAF was approximately 24 ns and that of Eu:LiSAF was about 1530 ns. These decay times are quite similar to those of Ce:LiCAF and Eu:LiCAF.

4. α-Ray and neutron-induced luminescence

The radio-luminescence spectra were investigated using the same spectrometer under 5.5 MeV α-ray excitation from ^{241}Am radio isotope. The α-ray excitation imitates the ^{6}Li(n, α)^{3}H reaction where charged particles excite the scintillator with high Q-value of 4.8 MeV. It must be noted that sometimes the emission peaks in the photo- and radio-luminesccence differ and to investigate radio-luminescence is important to choose appropriate photodetectors. A precise description of α-ray induced radio-luminescence was reported earlier [12]. Fig. 3 shows the radio-luminescence spectra of Ce 0.25, 0.50, 1.5, 2.0 and 3.0 mol% doped LiSAF scintillators. The intense emission peaks of Ce:LiSAF appeared at 315 and 335 nm due to the Ce^{3+} 5d–4f related transition. Due to the same reason as in the photoluminescence spectra, the emission peaks shifted to the longer wavelengths, as the concentration of Ce increased. Then, Eu 0.25, 0.50, 1.0, 2.0, 3.0 and 4.0 mol% doped LiSAF crystals showed one intense peak at 375 nm due to Eu^{2+} 5d–4f transition, as presented in Fig. 4, and it was in a good agreement with the photoluminescence measurements. With these experiments, the main emission peaks were experimentally determined under the radiation exposure. Based on their scintillation emission wavelengths, we choose the R7600 photomultiplier tube for the neutron induced light yield and decay kinetics experiments.

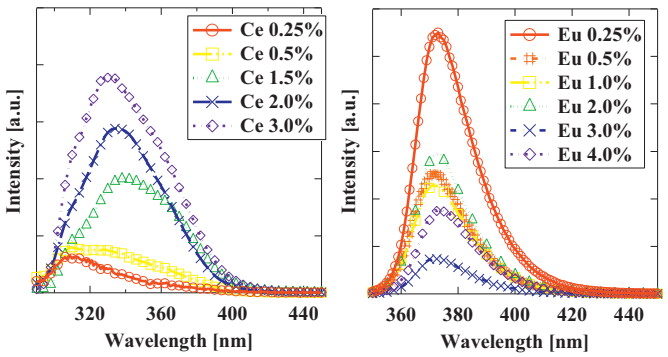

Fig. 2. Photoluminescence spectra of Ce:LiSAF (left) and Eu:LiSAF (right) under 280 and 330 nm excitation, respectively.

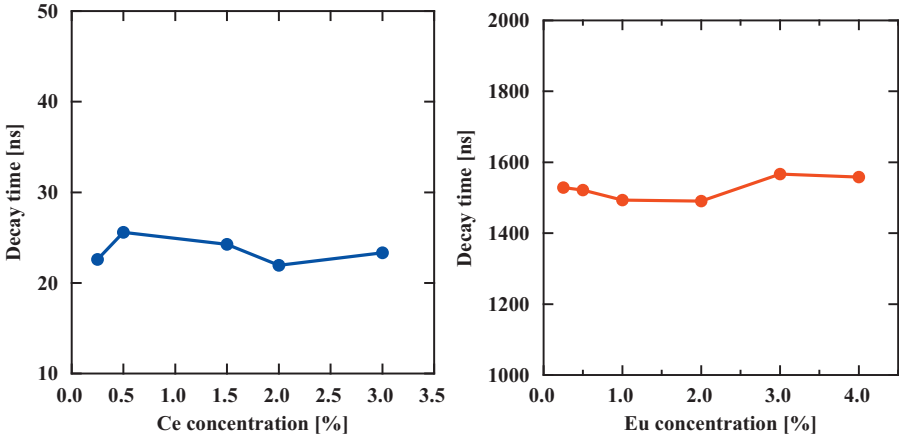

Fig. 3. Photoluminescence decays of Ce:LiSAF (left) and Eu:LiSAF (right) under 280 and 330 nm excitation, respectively.

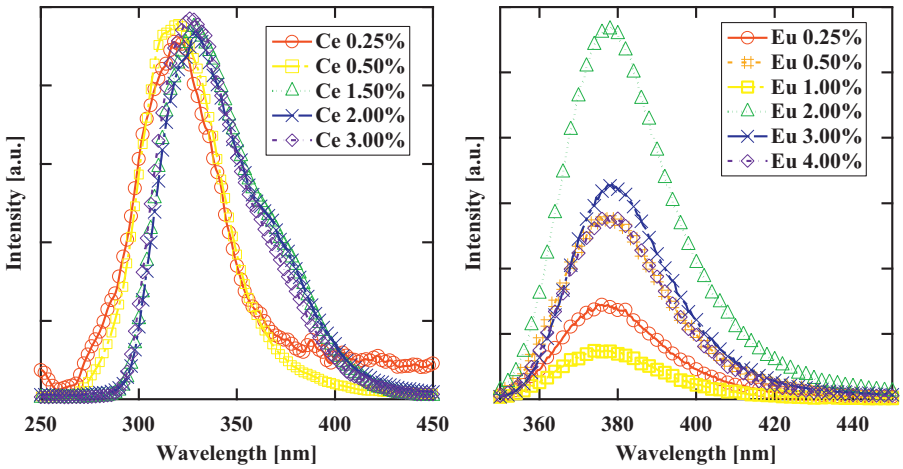

Fig. 4. Radioluminescence spectra of Ce:LiSAF (left) and Eu:LiSAF (right) under ^{241}Am α-ray excitation.

In order to confirm that α-ray induced radio-luminescence well simulates the neutron response, we have measured the neutron-induced radio-luminescence spectra. Because the machine time was limited, Eu 2%:LiSAF and Ce 3% LiSAF, which were the brightest samples among the studied LiSAFs were chosen. In the thermal neutron spectroscopy, the MUSASI (Multi-Purpose Thermal Neutron application and Science) beam port in JRR-3 was used as the 13.5 meV thermal neutron source (Maximum neutron flux ~800,000 counts/s/cm^2). The sample was mounted on the optical fiber and was set in front of the beam port. The thermal-neutron-induced luminescence was transmitted through the optical fiber and fed in the CCD camera equipped with a spectrometer. The thermal neutron luminescence spectrum of Eu 2%:LiSAF is shown in Fig. 5. The emission peak was centered at 378 nm, which was almost the same position as for the peak in the the α-ray-induced radio-luminescence spectrum. In Ce:LiSAF, the signal was very weak and could not be detected.

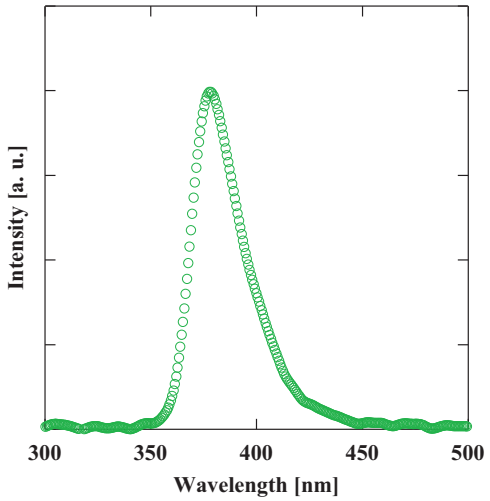

Fig. 5. Thermal-neutron-induced luminescence spectra of Eu 2%:LiSAF under thermal neutron excitation using MUSASI beam port in JRR-3.

5. Neutron responses

To determine the neutron light yield and scintillation decay time, the ^{252}Cf (< 3.7 MBq) was used as the neutron source. It was surrounded by 43 mm thick polyethylene layer as the moderator and reflector. The sample was mounted on the PMT (Hamamatsu, R7600) with silicon grease (OKEN 6262A) and covered with the 50 mm thick lead block to reduce background γ-ray. In order to obtain the pulse-height spectra under the thermal neutron excitation, we used a pre-amplifier (ORTEC 113), a shaping amplifier (ORTEC 572) with a shaping time of 3 μs and a multichannel analyzer (Amptek, Pocket MCA 8000A) in the pulse-height mode. Li-glass scintillator GS20 was used as a reference and the thermal neutron peak appeared at 464 ch in

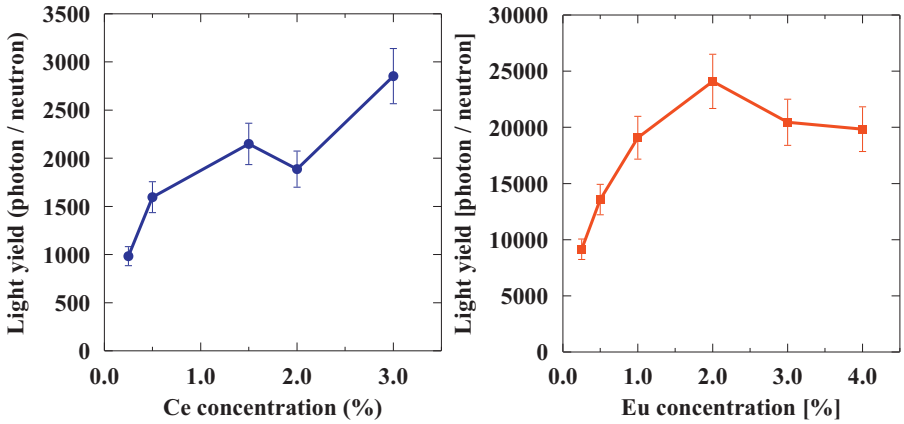

Fig. 6. Light yield of Ce:LiSAF (left) and Eu:LiSAF (right) under neutron irradiation plotted against Ce and Eu concentration, respectively.

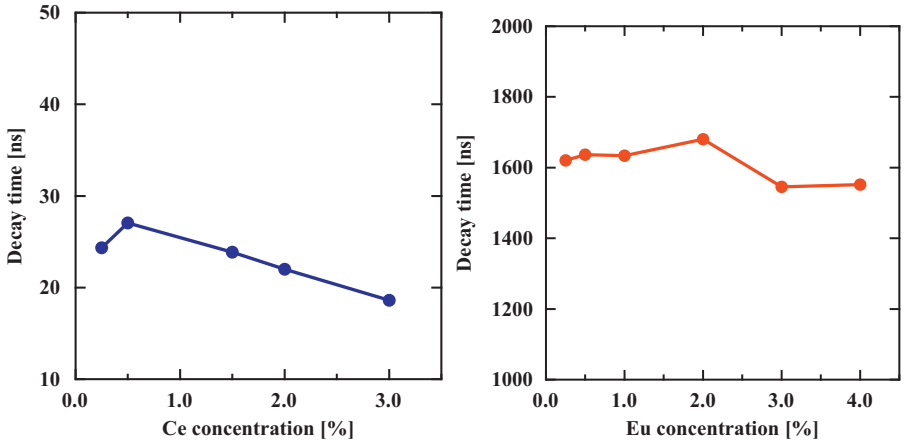

Fig. 7. Neutron-excited scintillation decays of Ce:LiSAF (left) and Eu:LiSAF (right).

this setup. In the pulse height spectra, we could observe thermal neutron peaks for all the samples.

The quantum efficiency of the used photomultiplier at approximately 375 nm (emission peak of EuLiSAF) is 45% and at 300 nm (emission peak of Ce:LiSAF) is 35%. The light yields of the LiSAF samples were calculated from the pulse height spectra of the thermal neutron peaks compared with that of Li-glass. For example, the peak channel of Ce 3 mol% LiSAF was 172 ch, and the light yield was calculated as 6000 ph/n (Light yield of GS20 [13]) × 172 ch/464 ch × 45%/35% = 2860 ph/n. Fig. 6 represents the light yield as a function of the Ce and Eu concentrations. The Ce 3%:LiSAF sample showed the highest light yield (2860 ph/n) among all the Ce:LiSAFs. Thus, the higher Ce doping concentration could lead to even higher light yield, but the transmittance would be worse due to the secondary phase. In the same manner, the light yield of Eu:LiSAFs was calculated and plotted as a function of the Eu concentration. The highest light yield for Eu:LiSAF was found to be 24,000 ph/n for the 2.0% doped sample and remained constant over 2.0%. These light yields are lower than those of Eu doped LiCAFs, because the secondary phase reduces the emission intensity of the crystals.

The thermal-neutron-excited scintillation decays were measured by 20 times integration of anode signal from PMT using digital oscilloscope and decay times were deduced by an exponential fitting. The thermal neutron scintillation decays of the Ce:LiSAF and Eu:LiSAF are summarized in Fig. 7. The decay time constants of Ce:LiSAFs decrease from 27 to 19 ns as the dopant concentration increased. They were slightly shorter than those of Ce:LiCAF. On the other hand, Eu:LiSAF showed 1610–50 ns when Eu concentration was below 2%. Eu 3% and 4% doped LiSAFs exhibited faster decay than the other Eu:LiSAFs. These values are equal to those of Eu:LiCAF.

6. Conclusion

In order to develop a neutron scintillation material to replace ^{3}He-based detectors, Ce and Eu doped LiSAF crystals with different dopant concentrations were grown by the μ-PD method. However, they included the secondary phase and the opacity was observed in higher dopant concentrations. In the photo- and radio-luminescence spectra of Ce:LiSAF, the peaks due to Ce^{3+} 5d–4f transition were observed at around 315 and 335 nm, and one peak around 375 nm due to Eu^{2+} 5d–4f transition was observed in the Eu:LiSAF. The positions of the peaks correspond to those in the spectra of their LiCAF-based analogs. The maximum neutron light yields are 2860 ph/n for Ce:LiSAF and 24,000 ph/n for Eu:LiSAF. They are smaller than those of LiCAF, because the opacity reduces the emission intensity of the crystals. The thermal neutron scintillation decay times are from 27 to 19 ns for Ce:LiSAF, and about 1610 ns for Eu:LiSAF. In the future work, we will control the impurity phase and prepare fully transparent samples to achieve higher light yield by the conventional Czochralski method, which can be generally used for high quality crystal growth.

Acknowledgment

This work was mainly supported by JST Sentan and partially by a Grant in Aid for Young Scientists (B)-15686001, (A)-23686135,

and Challenging Exploratory Research-23656584 from the Ministry of Education, Culture, Sports, Science and Technology of the Japanese government (MEXT). Partial assistance from the Yazaki Memorial Foundation for Science and Technology, Japan Science Society, Sumitomo Foundation, and Iketani Science and Technology Foundation are also gratefully acknowledged.

References

[1] R.T. Kouzes, J.H. Ely, L.E. Erikson, W.J. Kernan, A.T. Lintereur, E.R. Siciliano, D.L. Stephens, D.C. Stromswold, R.M. Van Ginhoven, M.L. Woodring, Nuclear Instruments and Methods in Physics Research A 623 (3) (2010) 1035.
[2] A. Yoshikawa, T. Yanagida, Y. Yokota, N. Kawaguchi, S. Ishizu, K. Fukuda, T. Suyama, K.J. Kim, J. Pejchal, M. Nikl, K. Watanabe, M. Miyake, M. Baba, K. Kamada, IEEE Transactions on Nuclear Science NS-56 (2009) 3796.
[3] T. Yanagida, A. Yoshikawa, Y. Yokota, S. Maeo, N. Kawaguchi, S. Ishizu, K. Fukuda, T. Suyama, Optical Materials 32 (2) (2009) 311.
[4] T. Yanagida, N. Kawaguchi, Y. Fujimoto, K. Fukuda, Y. Yokota, A. Yamazaki, K. Watanabe, J. Pejchal, A. Uritani, T. Iguchi, A. Yoshikawa, Optical Materials 33 (2011) 1243.
[5] T. Yanagida, N. Kawaguchi, Y. Fujimoto, Y. Yokota, A. Yamazaki, K. Watanabe, K. Kamada, A. Yoshikawa, V. Chani, Radiation Measurements, in press, doi: 10.1016/j.radmeas.2011.04.034.
[6] M. Kirm, Y. Chen, S. Neicheva, K. Shimamura, N. Shiran, M. True, S. Vielhauer, Physica Status Solidi C 2 (1) (2005) 418.
[7] N. Shiran, A. Gektina, S. Neichevaa, V. Voronovaa, V. Kornienkoa, K. Shimamurab, N. Ichinose, Radiation Measurements 38 (4–6) (2004) 459.
[8] N. Shiran, A. Gektin, S. Neicheva, M. Weber, S. Derenzo, M. Kirm, M. True, I. Shpinkov, D. Spassky, K. Shimamura, N. Ichinos, Nuclear Instruments and Methods in Physics Research A 537 (1–2) (2005) 266.
[9] A. Yoshikawa, T. Satonaga, K. Kamada, H. Sato, M. Nikl, N. Solovieva, T. Fukuda, Journal of Crystal Growth 270 (2004) 427.
[10] M. Nikl, Physica Status Solidi A 178 (2000) 595.
[11] M. Nikl, C. Pedrini, Solid State Communications 90 (1994) 155.
[12] T. Yanagida, K. Kamada, Y. Fujimoto, Y. Yokota, A. Yoshikawa, H. Yagi, T. Yanagitani, Nuclear Instruments and Methods in Physics Research A 631 (2011) 54.
[13] C.W.E. van Eijik, Radiation Measurements 38 (2004) 337.